AGU PUBLICATIONS

JGR

Journal of Geophysical Research: Space Physics

RESEARCH ARTICLE

10.1002/2017JA024415

Special Section:
Magnetospheric Multiscale (MMS) mission results throughout the first primary mission phase

Key Points:
- Kinetic-size magnetic holes are statistical investigated by MMS
- Observed kinetic-size magnetic holes seem to be best explained as electron vortex magnetic holes
- Kinetic-size magnetic holes are likely to heat and accelerate the electrons

Correspondence to:
S. Y. Huang,
shiyonghuang@whu.edu.cn

Citation:
Huang, S. Y., et al. (2017), A statistical study of kinetic-size magnetic holes in turbulent magnetosheath: MMS observations, *J. Geophys. Res. Space Physics*, *122*, 8577–8588, doi:10.1002/2017JA024415.

Received 31 MAY 2017
Accepted 12 AUG 2017
Accepted article online 16 AUG 2017
Published online 29 AUG 2017

A statistical study of kinetic-size magnetic holes in turbulent magnetosheath: MMS observations

S. Y. Huang[1], J. W. Du[1], F. Sahraoui[2], Z. G. Yuan[1], J. S. He[3], J. S. Zhao[4], O. Le Contel[2], H. Breuillard[2], D. D. Wang[1], X. D. Yu[1], X. H. Deng[5], H. S. Fu[6], M. Zhou[7], C. J. Pollock[8], R. B. Torbert[9], C. T. Russell[10], and J. L. Burch[11]

[1]School of Electronic Information, Wuhan University, Wuhan, China, [2]Laboratoire de Physique des Plasmas, CNRS-Ecole Polytechnique-UPMC, Palaiseau, France, [3]School of Earth and Space Sciences, Peking University, Beijing, China, [4]Key Laboratory of Planetary Sciences, Purple Mountain Observatory, Chinese Academy of Sciences, Nanjing, China, [5]Institute of Space Science and Technology, Nanchang University, Nanchang, China, [6]School of Space and Environment, Beihang University, Beijing, China, [7]Department of Physics and Astronomy, University of California, Los Angeles, California, USA, [8]NASA Goddard Space Flight Center, Greenbelt, Maryland, USA, [9]Physics Department, University of New Hampshire, Durham, New Hampshire, USA, [10]Department of Earth, Planetary and Space Sciences, University of California, Los Angeles, California, USA, [11]Southwest Research Institute, San Antonio, Texas, USA

Abstract Kinetic-size magnetic holes (KSMHs) in the turbulent magnetosheath are statistically investigated using high time resolution data from the Magnetospheric Multiscale mission. The KSMHs with short duration (i.e., $<$0.5 s) have their cross section smaller than the ion gyroradius. Superposed epoch analysis of all events reveals that an increase in the electron density and total temperature significantly increases (resp. decrease) the electron perpendicular (resp. parallel) temperature and an electron vortex inside KSMHs. Electron fluxes at ~90° pitch angles with selective energies increase in the KSMHs are trapped inside KSMHs and form the electron vortex due to their collective motion. All these features are consistent with the electron vortex magnetic holes obtained in 2-D and 3-D particle-in-cell simulations, indicating that the observed KSMHs seem to be best explained as electron vortex magnetic holes. It is furthermore shown that KSMHs are likely to heat and accelerate the electrons.

Plain Language Summary A nonlinear energy cascade in magnetized turbulent plasmas leads to the formation of different coherent structures which are thought to play an important role in dissipating energy and transporting particles. This study statistically investigate one new type of coherent structure, named electron vortex magnetic hole, used by Magnetospheric Multiscale data. It reveals the common features of this structure, including an increase in the electron density and total temperature, significantly increase (resp. decrease) the electron perpendicular (resp. parallel) temperature and an electron vortex inside these holes. The increase of electron temperature inside the holes indicates that these holes are likely to heat and accelerate the electrons. This gives new clue for energy dissipation in turbulent plasmas.

1. Introduction

Magnetic holes, characterized by significant magnetic depression, are widely observed in space including the solar wind [e.g., *Turner et al.*, 1977; *Zhang et al.*, 2009], planetary magnetosheaths [e.g., *Violante et al.*, 1995; *Tsurutani et al.*, 2011], cusp region [e.g., *Shi et al.*, 2009], and plasma sheet [e.g., *Ge et al.*, 2011; *Balikhin et al.*, 2012]. The spatial scales of the magnetic holes can vary from several ρ_i (ion gyroradius) to thousands of ρ_i. There are various mechanisms for the generation of such large-scale magnetic holes: mirror instabilities [*Tsurutani et al.*, 1982; *Fazakerley and Southwood*, 1994; *Chisham et al.*, 1999; *Horbury et al.*, 2004; *Zhang et al.*, 2008, 2009; *Shi et al.*, 2009], sheet-like equilibrium structures [*Burlaga and Lemaire*, 1978], solitons derived within the Hall MHD theory [e.g., *Baumgärtel*, 1999; *Stasiewicz*, 2004], and theories associated with Alfvén waves [e.g., *Tsurutani et al.*, 2005].

Recently, small-scale magnetic holes (less than ion gyroradius) have been detected in the plasma sheet [*Sun et al.*, 2012; *Sundberg et al.*, 2015; *Gershman et al.*, 2016; *Goodrich et al.*, 2016]. These small-scale magnetic holes cannot be explained by the aforementioned mechanisms. Based on the electron magnetohydrodynamic (EMHD) theory with Biermann battery effect, electron magnetosonic solitons are used to explain those small-scale magnetic holes [*Ji et al.*, 2014; *Li et al.*, 2016; *Yao et al.*, 2016]. Recent 2-D

and 3-D particle in-cell (PIC) simulations have revealed a new type of subproton-scale magnetic hole with trapped electrons that form the electron vortex during the evolution of turbulence, also named "electron vortex magnetic hole," which can explain the observed properties of small-scale magnetic holes in the magnetotail plasma sheet [*Haynes et al*., 2015; *Roytershteyn et al*., 2015]. More recently, using in situ high time resolution data from the Magnetospheric Multiscale (MMS) mission, electron vortex magnetic holes were identified in the turbulent magnetosheath [*Huang et al*., 2017a; *Yao et al*., 2017]. In this paper we refer to those small-scale magnetic holes by kinetic-size magnetic holes (KSMHs).

The magnetosheath, the region bounded by the bow shock and the magnetopause, is highly dynamical and exhibits a variety of dynamical features such as heating and compression of the plasma, kinetic instabilities, particle beams, and kinetic structures [*Sahraoui et al*., 2003, 2004, 2006; *Karimabadi et al*., 2014; *He et al*., 2011; *Huang et al*., 2012, 2014, 2017b; *Yordanova et al*., 2008; *Tsurutani et al*., 2011; *Breuillard et al*., 2016]. It provides a natural environment to study kinetic structures, such as reconnecting current sheet [*Retinò et al*., 2007], ion and electron scale magnetic structures [*Huang et al*., 2016, 2017a; *Yao et al*., 2017]. In this paper, we investigate the statistical properties of KSMHs in the magnetosheath based on the unprecedented high-resolution measurements from MMS mission [*Burch et al*., 2015].

The layout of this paper is as follows: the procedure we used to select the data related to KSMHs are given in section 2, the case and statistical results are shown in section 3, the generation mechanisms are discussed in section 4, and finally, a summary of the study is presented in section 5.

2. MMS and Data Procedure

2.1. MMS

The MMS mission was launched on 12 March 2015 and consists of four identical spacecraft [*Burch et al*., 2015]. Science operations began in September 2015. The four spacecraft form a tetrahedron with separation distance of about 10 km in the science phase 1. MMS provides very high time resolution measurements of fields and particles [*Burch et al*., 2015]. In the present study, we used magnetic field data measured by the Fluxgate Magnetometer instruments with the sampling frequency of 128 Hz in the burst mode [*Russell et al*., 2016], the 3-D particle velocity distribution functions, and the plasma moments from the Fast Plasma Instrument sampled at 30 ms for electrons and 150 ms for ions in burst mode [*Pollock et al*., 2016].

2.2. Data Procedure

We surveyed MMS burst mode data in the magnetosheath from September 2015 to January 2016 (5 month period). Following *Zhang et al*. [2008], the criterion used to identify magnetic holes is that the amplitude depression (B_{min}/B) is smaller than 0.75, where B_{min} is the minimum magnetic field magnitude inside a magnetic hole and B is the average magnetic field magnitude in a given time interval. To avoid selecting current sheets that can fulfill this criterion, we chosed only time intervals when the magnetic field vectors at the two boundaries of a magnetic hole change by less than 15°. We used a window of 2 s short time interval to survey kinetic-size magnetic holes because the magnetic field in the magnetosheath can exhibit large fluctuations and target magnetic holes that have durations less than 0.5 s. Our data selection resulted in a total of 66 KSMH events.

3. MMS Observations of KSMHs in the Magnetosheath

3.1. Case Study

An overview plot of an example of the identified KSMH on 14 September 2015 is shown in Figure 1. Magnetic amplitude depression B_{min}/B of the hole is about 0.48. The hole is observed around 12:28:49.08 UT with a duration of 0.164 s. Only electron measurements are shown in Figure 1 considering the short duration of the hole and low time resolution of ion data. We can see that electron density (Figure 1c), total temperature (Figure 1d), and perpendicular temperature (Figure 1f) increase in KSMH, while electron parallel temperature decreases. The magnetic field data and electron velocity are presented in *LMN* coordinates (Figures 1b and 1h–1j), which is determined by minimum variance analysis of the magnetic field [*Sonnerup and Scheible*, 1998]. In this coordinate system, the maximum variation direction **L** can be considered as the axis of the magnetic hole and the intermediate variation direction **M** and the minimum variation direction **N** are in the cross section of the magnetic hole. During the crossing of KSMH, V_{em} and V_{en} components of electron

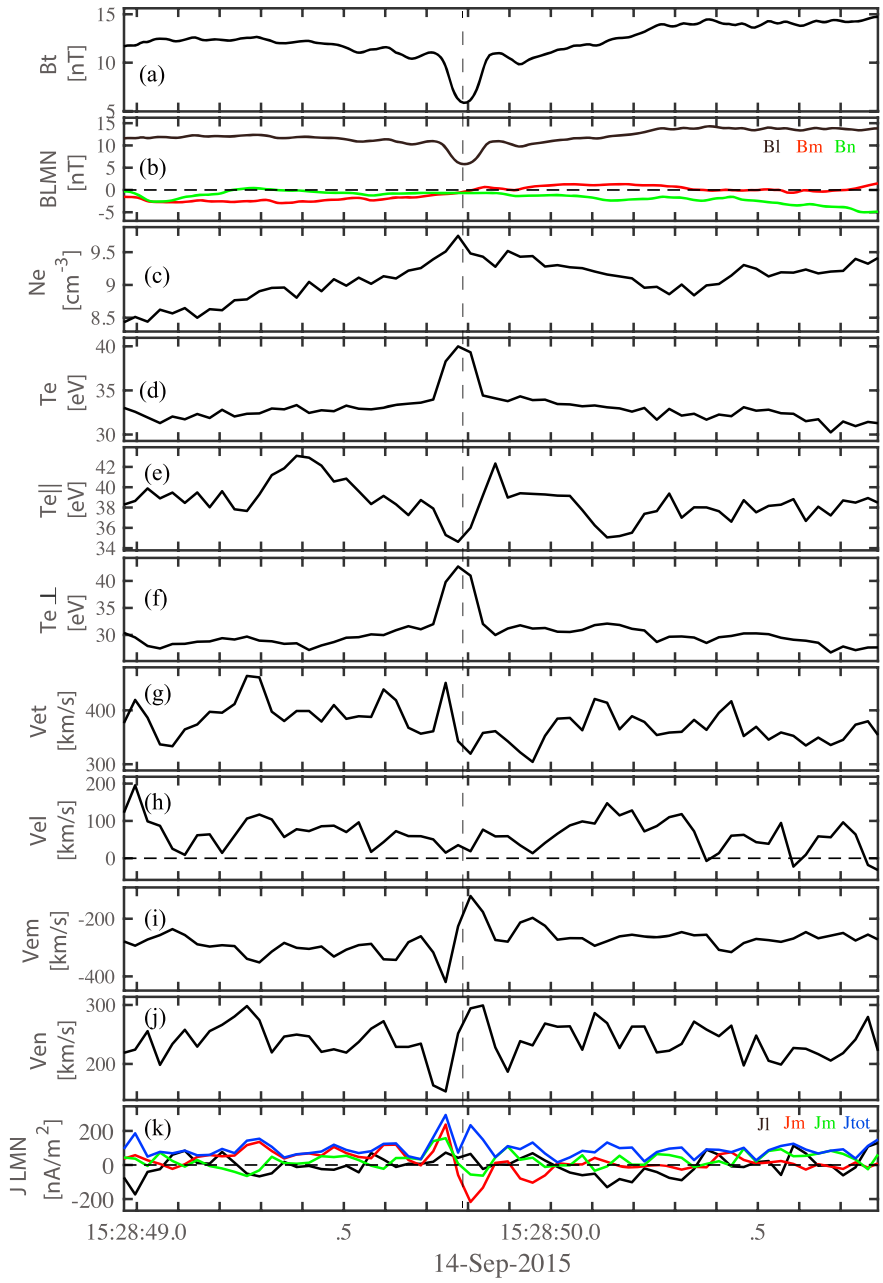

Figure 1. Detailed observations of a case study of KSMH in the magnetosheath (vector data are given in *LMN* coordinates). (a and b) Magnitude and three components of the magnetic field. (c) Electron density, (d) total temperature, (e) parallel temperature, and (f) perpendicular temperature. (g–j) Magnitude and three components of the electron velocity, and (k) current density. The black dashed line marks the minimum of magnetic field.

velocities (Figures 1i and 1j) exhibited a bipolar variation on the comoving frame of the background flow, implying the possible existence of an electron vortex structure in the *M-N* plane inside the magnetic hole similar to the one simulated in *Haynes et al*. [2015] and observed by *Huang et al*. [2017a]. The current is estimated using the plasma measurements (i.e., $\boldsymbol{J} = ne(\boldsymbol{V}_i - \boldsymbol{V}_e)$, where n is the plasma density, e is the electric charge, $\boldsymbol{V}_i$ is the ion flow, and $\boldsymbol{V}_e$ is the electron flow). The current is also presented in *LMN* coordinates in Figure 1k. Currents are intense in the KSMH. Bipolar signature in the J_m and J_n components is similar but with opposite sign than the electron velocity component V_{em} and V_{en}. Thus, one can deduce that electrons carry most of the electric current inside KSMH. MMS observed a dip in the total current in

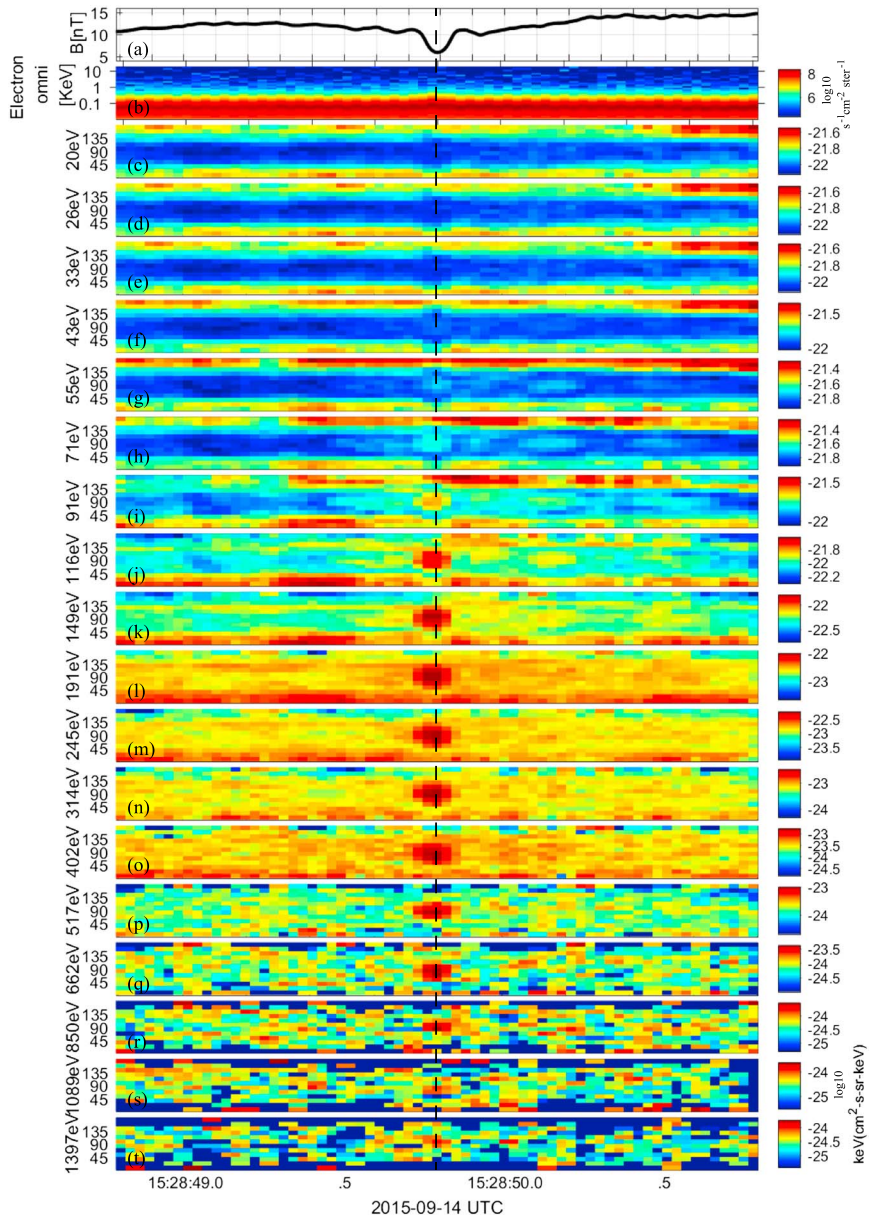

Figure 2. Electron observations of KSMH in the magnetosheath. (a) Magnitude of the magnetic field. (b) Omni-directional electron fluxes, (c–t) Electron pitch angle distributions. The black dashed line marks the minimum of the magnetic field.

the middle of the hole, which is similar to previous simulations results that showed a dip in the core region of magnetic hole [*Haynes et al.*, 2015]. This suggests that MMS was close to the center of the KSMH. The assumption that the magnetic hole moves with the ambient plasma flow is used to estimate the scale of the magnetic hole in the *M-N* plane. The width of the magnetic hole is about 60 km, which was estimated using the equation $D_N = |V_e| \times dt$, where $|V_e| \approx 362$ km/s is the averaged electron velocity in *M-N* plane, and $dt \approx 0.164$ s is the duration of the crossing of the hole. The estimated size is about 0.21 ρ_i (~37 ρ_e), where ρ_i and ρ_e are the proton and electron gyroradii (ρ_i ~ 289 km and ρ_e ~ 1.59 km based on $|B|$ ~ 12 nT, n ~ 9 cm^{-3}, T_i ~ 624 eV and T_e ~ 34 eV).

Figure 2 shows the electron omni-directional fluxes and pitch angle distributions. The electron fluxes are slightly enhanced inside KSMH (Figure 2b). The perpendicular electron phase space densities significantly increase in the energy range from 55 eV to 850 eV inside KSMH (Figures 2h–2r), while they show no clear enhancements or are stable for energies <55 eV or >850 eV. This implies that electrons having energy

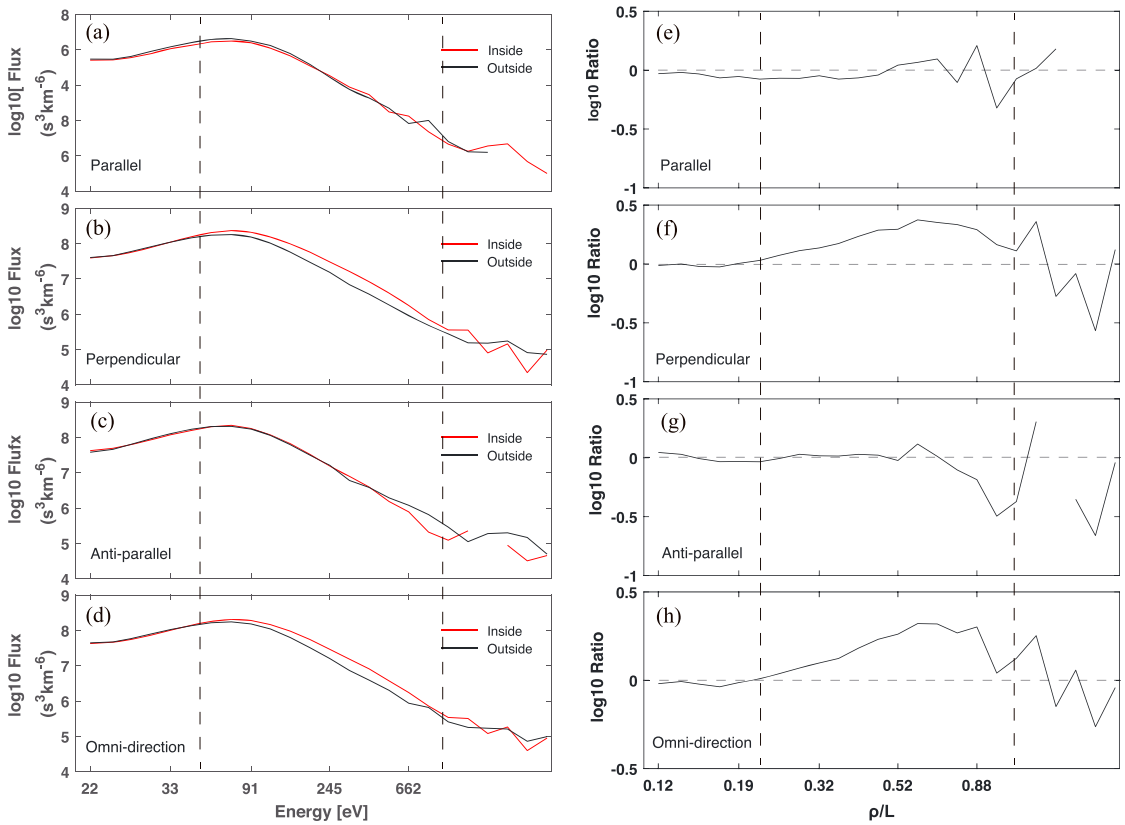

Figure 3. (a–d) Comparisons between electron fluxes inside KSMH and outside KSMH as function of the energy, and (e–h) their ratios as function of the electron gyroradius normalized by the width of KSMH. Minimum and maximum values of the energy and gyroradius of the trapped electrons are indicated by the vertical dashed lines.

from 55 to 850 eV are trapped inside the KSMH. To clearly demonstrate this phenomenon, we show in Figure 3 the electron parallel, perpendicular, antiparallel, and omni-directional fluxes inside and outside KSMH. One can see that parallel and antiparallel fluxes are more or less located both inside and outside of the KSMH (Figures 3a and 3c), while perpendicular fluxes inside of KSMH are higher than those outside of KSMH in the energy range of 55–805 eV (marked by two dashed lines). The ratios of electron fluxes inside and outside of KSMH are shown in Figures 3e–3h as function of the electron gyroradius normalized to the width of KSMH. It clearly demonstrates a similar feature that the perpendicular fluxes increase inside of KSMH compared with those outside of KSMH, which lead the enhancement of electron omni-directional fluxes inside of KSMH. It is interesting to note that the increased electron perpendicular fluxes have limited energies, implying that only part of electrons can be trapped in the KSMH as revealed by the simulations of *Haynes et al*. [2015].

3.2. Statistical Results

In this section we analyze all the 66 KSMH events that resulted from our data selection. Figure 4 displays the width of KSMHs normalized by ion gyroradius ρ_i and electron gyroradius ρ_e. One can see that the scales of all magnetic holes are less than one ion gyroradius (Figure 4a), or tens of the electron gyroradius (Figure 4b), thus demonstrating that these holes are kinetic-size structures.

To obtain some common features of the KSMHs, we performed superposed epoch analysis of all KSMH events during the interval from 1 s before to 1 s after the time when the minimum magnetic field magnitude is observed. From top to bottom in Figure 5, B_t, N_e, T_e, $T_{e\|}$, $T_{e\perp}$, and V_{em} (or V_{en}) are plotted. For all parameters, averaged value has been subtracted. If V_{em} or V_{en} has one positive-negative bipolar variation, the variation of V_{em} or V_{en} will be changed to negative-positive bipolar in order to conveniently display the results. The red solid lines are the averaged values of the magnetic field and electron parameters. The magnetic field

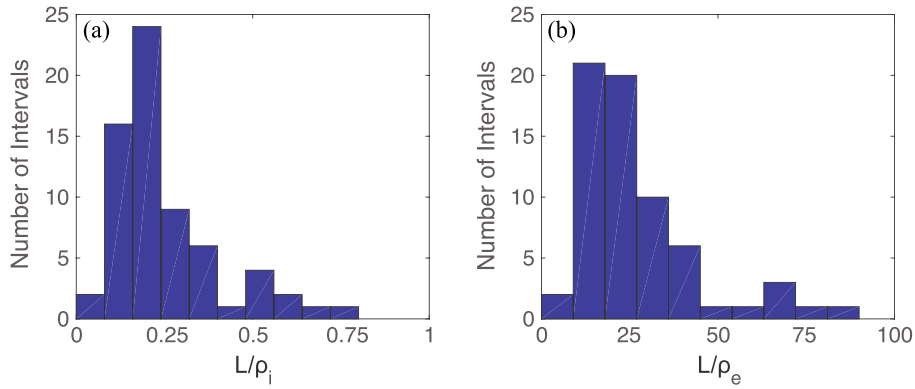

Figure 4. Histograms of the ratios of KSMH scale sizes to (a) ion gyroradius and (b) electron gyroradius.

magnitude B_t has a dip with the duration less than 0.2 s. Electron density has a slight enhancement, and electron temperature has a clear increase in the KSMHs. However, the electron parallel temperature $T_{e\|}$ always decreases, but the electron perpendicular temperature $T_{e\perp}$ significantly increases, similar to the case study. All electron velocity components V_{em} or V_{en} have a bipolar signature, implying the existence of an electron vortex inside KSMHs. These statistical results are consistent with the previous case study and with the results of *Huang et al*. [2017a] and *Yao et al*. [2017]. In addition, we also quantitatively calculate the values of the increase or decrease ratios of electron parameters (for example $\delta N_e/N_e$). The averaged results reveal a moderate enhancement (~9.5%) of N_e and T_e, a strong enhancement (~33%) of $T_{e\perp}$ and a moderate decrease (~9.8%) of $T_{e\|}$.

Figure 6 displays the ratios of the electron fluxes inside and outside KSMHs at different pitch angles and different energies (color code reflects the number of events). One can clearly see that the electron fluxes inside KSMHs at low energy (≤55 eV; Figures 6a–6e) are stable; the electron fluxes at intermediate energy level (71–850 eV; Figures 6f–6p) significantly enhance at ~90° pitch angles for most of events; electron fluxes at high energy level (≥1089 eV) have large fluctuations, but most of events have decreasing electron fluxes inside KSMHs. Figure 7 displays the superposed epoch analysis of the ratios of the electron parallel, perpendicular, antiparallel, and omni-directional fluxes inside and outside KSMHs as function of the energy. The red solid lines present the averaged values, and the cyan lines label standard deviations. One can see that there are large fluctuations of the ratios at high energies. Electron parallel and antiparallel fluxes show no clear enhancements and have their ratio close to 1 inside and outside KSMHs (Figures 7a and 7c), while perpendicular fluxes inside of KSMHs are significantly higher than those outside of KSMHs in the intermediate energy range (Figure 7b) which leads to the similar enhancements in the electron omni-directional fluxes. This result clearly demonstrates that only a fraction of electrons with appropriate energy can be trapped and form electron vortices in the KSMHs.

4. Generation Mechanisms

Several generation mechanisms of KSMHs have been proposed that include electron mirror mode instabilities, field-swelling instabilities, electron magnetosonic solitons, and self-generations of electron vortex magnetic hole [e.g., *Gary and Karimabadi*, 2006; *Pokhotelov et al*., 2013, *Baumgärtel*, 1999; *Stasiewicz et al*., 2003; *Li et al*., 2016; *Haynes et al*., 2015; *Roytershteyn et al*., 2015].

The instability threshold of the linear mirror mode is given by $R = (T_\perp/T_\|)/(1 + 1/\beta_\perp) > 1$. In Figure 8, we present the distributions of ion and electron $\beta_\perp$ and temperature anisotropy $T_\perp/T_\|$ for all events to test the stability condition of ion and electron mirror modes. First, one can see in Figure 8b that all events lie near the isotropy condition of electrons ($T_{e\perp} \sim T_{e\|}$) and below the magenta curve of the threshold of electron mirror instability (R = 1), which would rule out the possibility that the observed KSMHs be generated by electron mirror instability. Figure 8a shows that about 45% of the observed KSMHs lie near (or above) the ion mirror instability curve. However, previous studies showed that the scale of magnetic depressions (or dips) generated by ion mirror instability is of the order of ion gyroradius [e.g., *Hasegawa*, 1969], while the scale

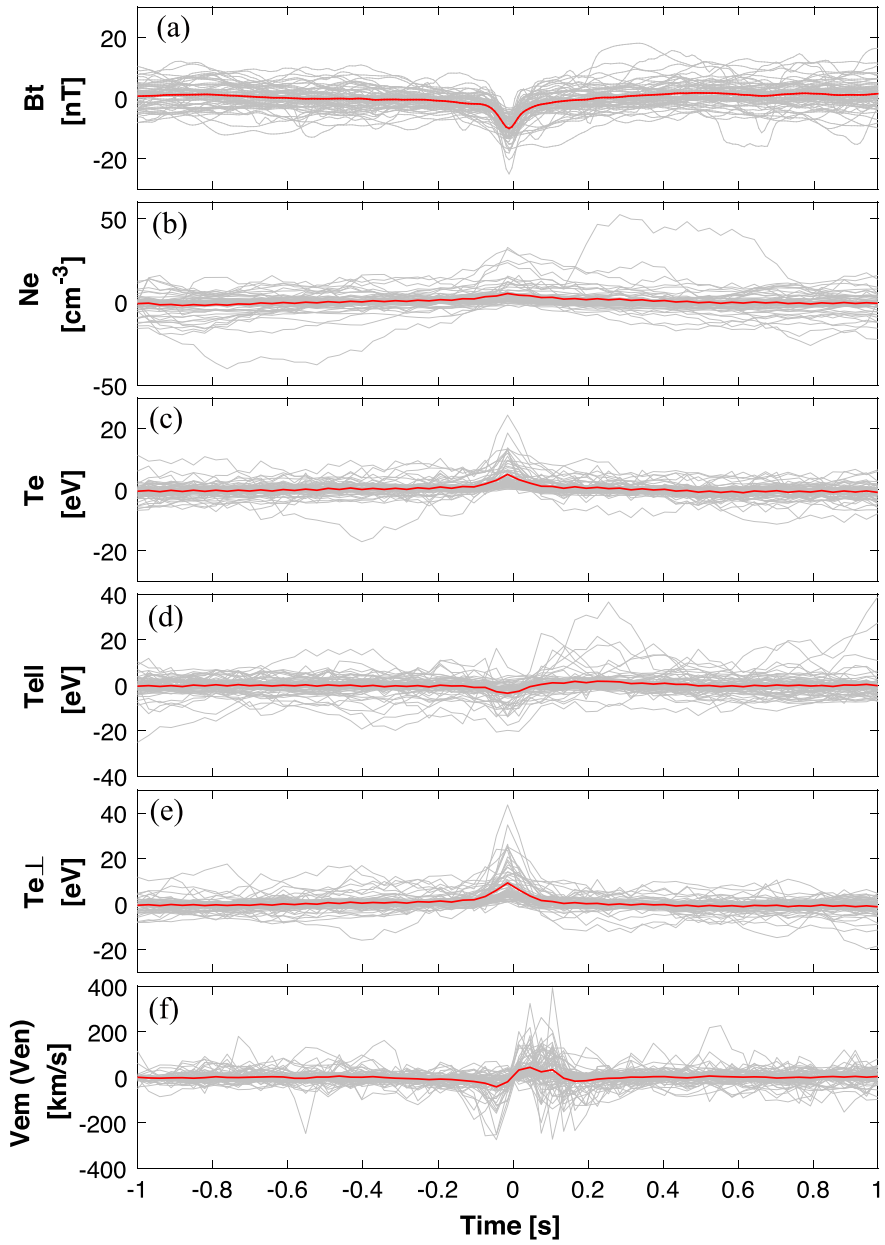

Figure 5. Superposed epoch analysis of all KSMH events during the interval from 1 s before t_0 to 1 s after t_0, where t_0 is the time when the minimum of magnetic field magnitude is observed: (a) B_t, (b) N_e, (c) T_e, (d) $T_{e||}$, (e) $T_{e\perp}$, and (f) V_{em} (or V_{en}). The red lines represent the average values of the corresponding data.

of the identified KSMHs is clearly below the ion gyroradius. Therefore, the role of ion mirror instability in generating the observed KSMHs is highly questionable [e.g., *Gary and Karimabadi*, 2006].

The field-swelling instability requires that the electron temperature be much larger than that of the ions [e.g., *Pokhotelov et al*., 2013]. Figure 9 displays the ratio between the ion and temperature both inside and outside KSMHs. It can be clearly seen that the ion temperature is twice the electron temperature. Only one event shows comparable values of the two temperatures. The field-swelling instability conditions are not met in the present data sets, and therefore, it could not have generated the observed KSMHs.

Regarding electron magnetosonic solitons obtained from a quasi-2-D EMHD model, the amplitude of the magnetic hole dB/B_0 has a linear dependence on the parameter characterizing the size of the magnetic

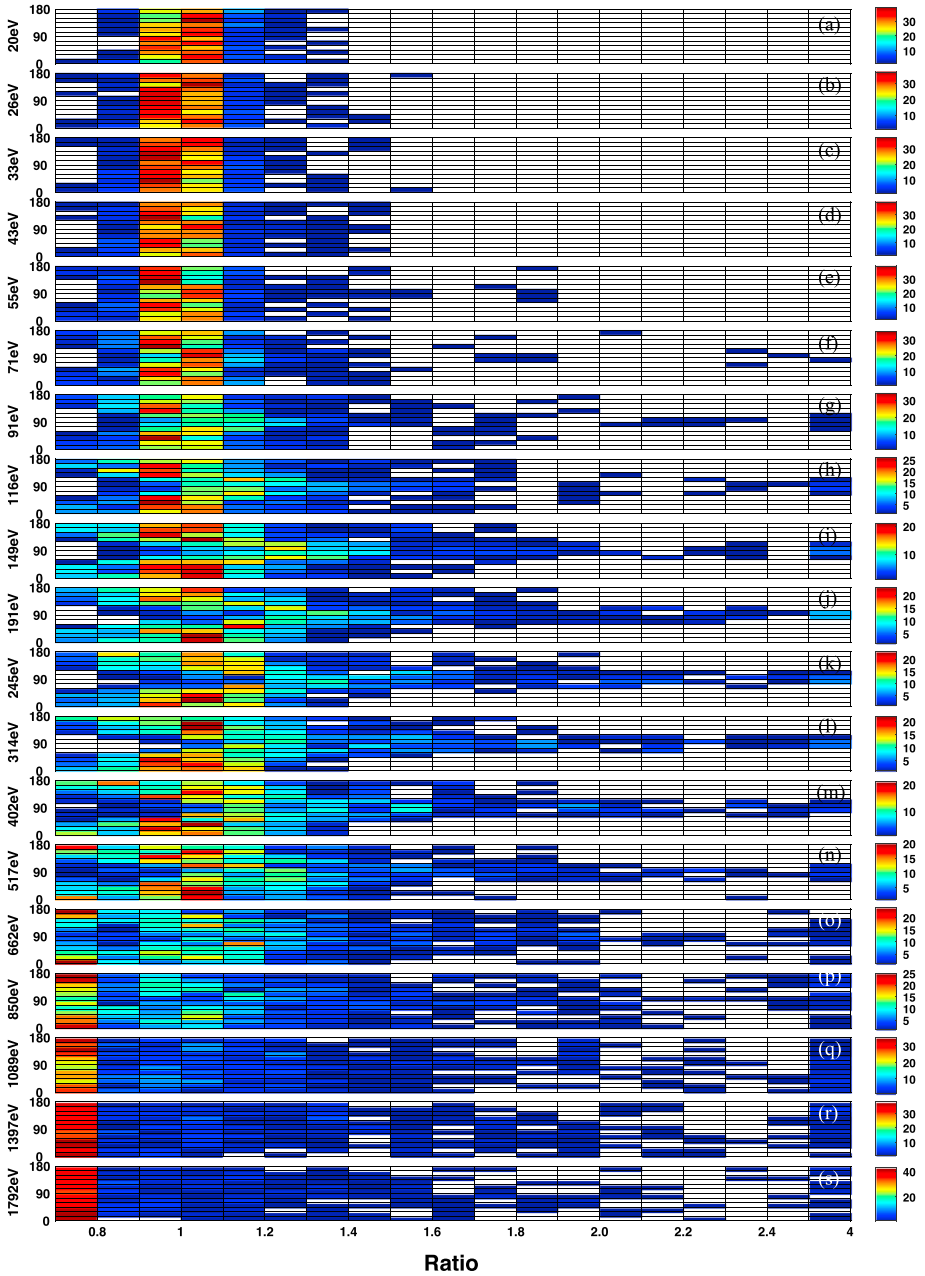

Figure 6. The ratios of electron fluxes inside and outside KSMHs with different pitch angles at different energies. The colors represent the number of KSMH events.

hole v [*Li et al.*, 2016; *Yao et al.*, 2016]. Testing this condition requires estimating the velocity of the KSMHs. However, the timing method cannot be used here to estimate the velocity of the KSMHs because the four MMS spacecraft did not observe the same KSMHs (their size being smaller than the spacecraft separation). Instead, we can use the width L of the magnetic hole which is proportional to $(-v)^{1/2}$ according to the results from *Li et al.* [2016], and therefore $v \propto 1/L^2$. Thus, the relation to test becomes $dB/B_0 \propto 1/L^2$. The results are displayed in Figure 10 and show no significant correlation (~0.18) between dB/B_0 and $1/L^2$. Based on the prediction from quasi-2-D EMHD model that showed that the magnetosonic solitons have size of ~10 ρ_e, we show in Figure 10 (in red color) the KSMHs with the scale size 10–20 ρ_e. Here too, the correlation (~0.3) is rather weak. In addition, the solitons are planar waves, implying that multispacecraft should detect the identical magnetic structures when they cross the holes. However, MMS spacecraft

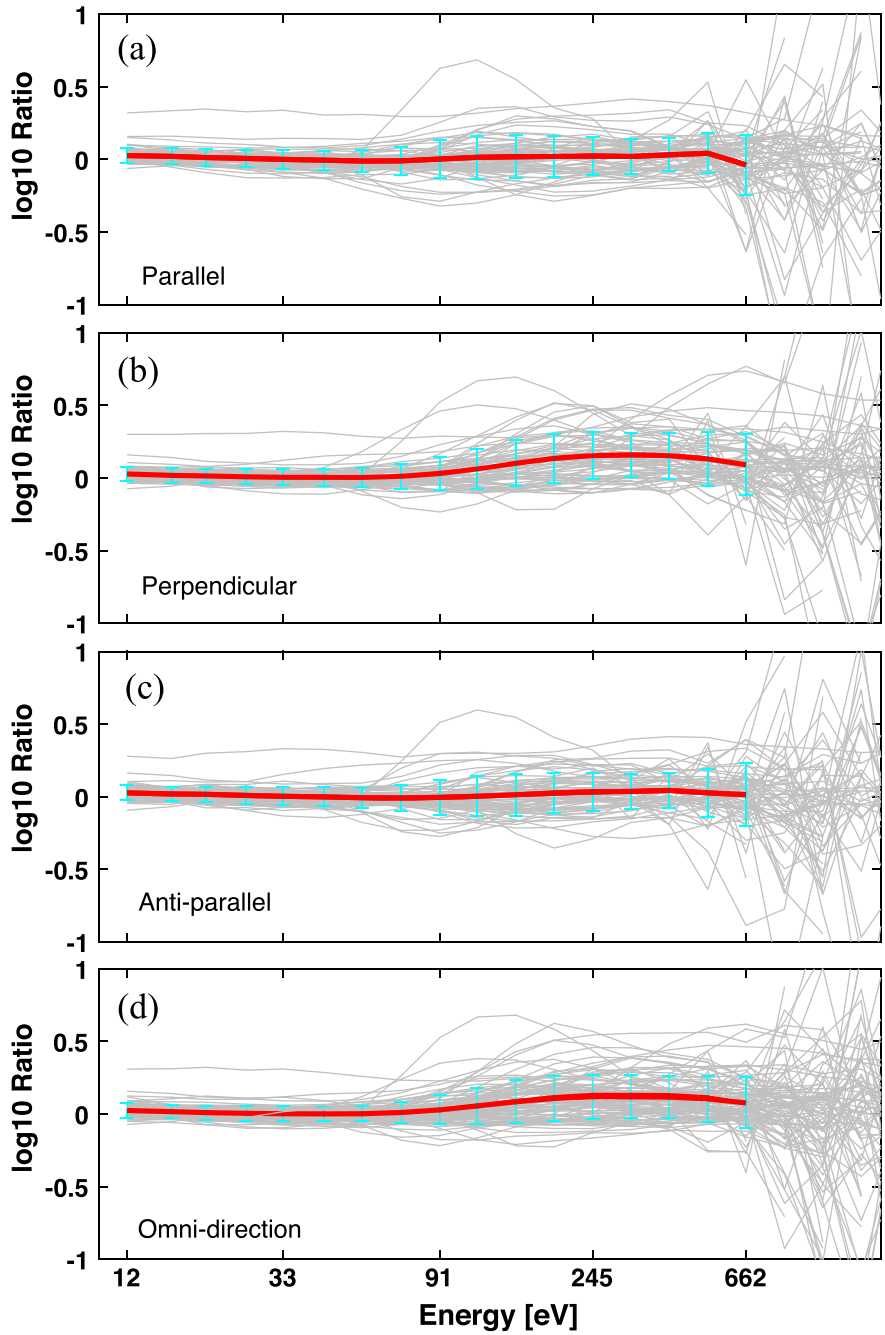

Figure 7. Superposed epoch analysis of the ratios of electron parallel, antiparallel, perpendicular, and omni-directional fluxes inside and outside KSMHs, respectively. The red solid lines present the averaged values, and the cyan lines display standard deviations.

observed different magnetic structures for most of KSMHs in present study. Thus, these clues indicate that the observed KSMHs may not be explained by the presented soliton theory.

Recently *Haynes et al.* [2015] and *Roytershteyn et al.* [2015] have shown using numerical simulations the existence of electron vortex magnetic holes as a new type of nonlinear coherent structure in turbulent magnetized plasmas. They reported several features of the electron vortex magnetic hole in agreement with our observations: size of the order of the electron scale (~0.18 ρ_i or ~12 ρ_e), trapped electrons to form the electron vortex, and an increase in electron density, temperature, and perpendicular temperature. *Haynes*

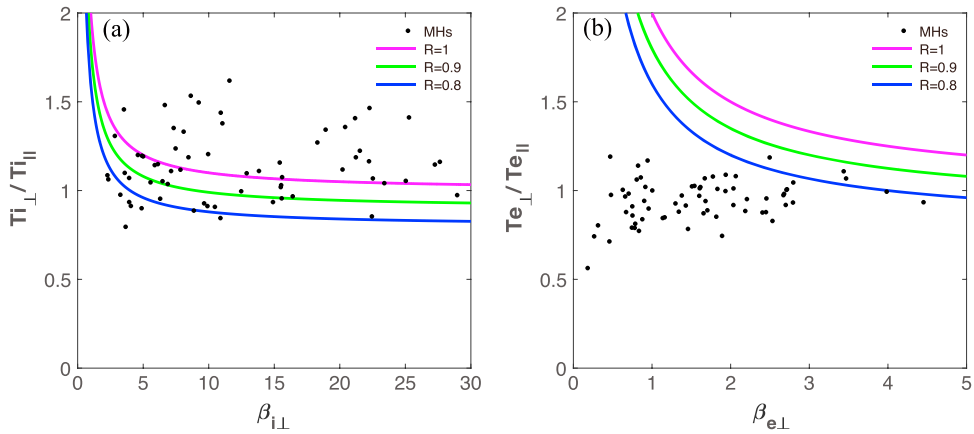

Figure 8. The distributions of $\beta_\perp$ and temperature anisotropy $T_\perp/T_{||}$ for all KSMH events detected by MMS for (a) the ions and (b) the electrons. The magenta curves represent the threshold of the linear mirror instability (R = 1); the green and blue curves show the values of R = 0.9 and R = 0.8, respectively.

et al. [2015] have traced the electron trajectories in their particle-in-cell and test particle simulations and found that the electron vortex magnetic holes have a preferred energy range of the trapped electrons with their gyroradius smaller than the hole's radius. It was suggested that the electron vortex is due to the collective motion of mean azimuthal trapped electron flow. It is interesting to note that in our study the electron perpendicular fluxes enhance only at selective energy band (~71–850 eV), in qualitative agreement with the simulations of *Haynes et al*. [2015]. Thus, our case and statistical study reveals the similar features as shown in the simulations, indicating that the observed KSMHs in the magnetosheath belong to electron vortex magnetic hole and can be explained by the simulations of *Haynes et al*. [2015] and *Roytershteyn et al*. [2015].

5. Summary

We have analyzed a series of 66 kinetic-size magnetic holes in the turbulent magnetosheath detected by the MMS spacecraft. The main features of the KSMHs are as follows:

1. Their scales are smaller than one ion gyroradius (or tens of electron gyroradius).
2. A moderately increase in electron density and temperature, a significantly increase in the electron perpendicular temperature, and a moderately decrease in the electron parallel temperature inside KSMHs.
3. Electron vortices, characterized by bipolar signature in one electron velocity component (V_{em} or V_{en}) in the cross section, are embedded in the KSMHs.
4. Electrons with selective energies are trapped and form the electron vortex inside KSMHs, which leads to an increase in the electron fluxes at ~90° pitch angles.
5. KSMHs seem to be best explained as electron vortex magnetic holes reported in earlier PIC simulations of the turbulent plasma.

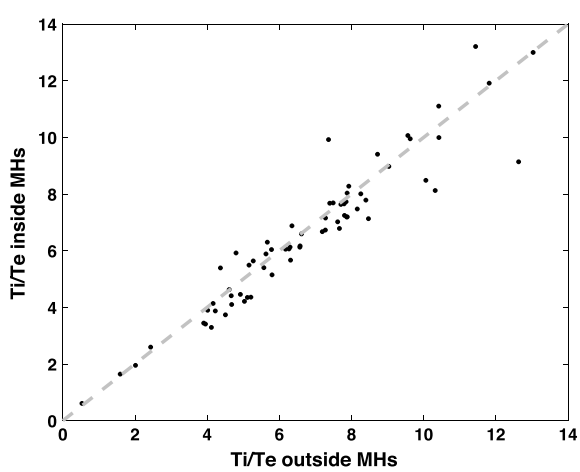

Figure 9. The distributions of T_i/T_e inside and outside KSMHs. The dashed line represents the linear relation ($y = x$).

Using the data from Ulysses spacecraft, *Tsurutani et al*. [2002] have found an increase in ion perpendicular temperature inside magnetic holes having scales as high as tens of ion gyroradius. They proposed that the ions were energized in the magnetic holes

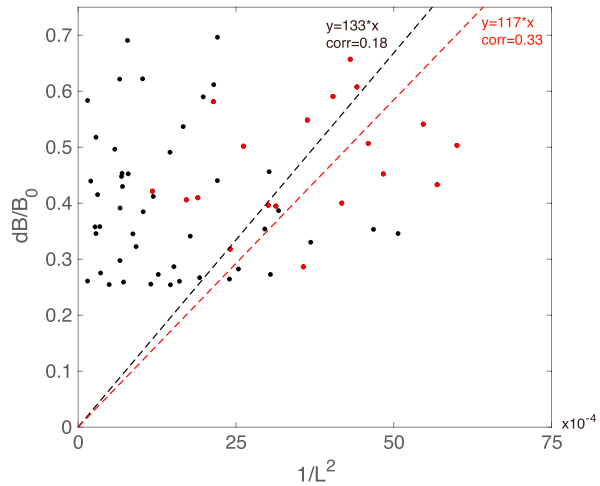

Figure 10. The distributions of dB/B_0 and $1/L^2$ for all KSMH events. The events with the scale size 10 ~ 20 ρ_e are marked by red points. The corresponding linear fits of all events (including both black and red points) and red point events are displayed by black dashed and red dashed lines, respectively.

by a ponderomotive force. In addition, *Russell et al.* [2008] proposed that the the magnetic holes carry on the information about heating and acceleration of the solar wind particles from the solar corona. Our present results indicate that the electron temperature and perpendicular temperature increase (up to 33%) inside KSMHs. This may indicate that electrons can be heated and accelerated in the KSMHs. Numerical modeling and simulations are needed to elucidate those physical processes of heating and acceleration of electrons within the KSMHs. We will investigate the electron acceleration/heating mechanisms within KHMSs in future.

Acknowledgments
We thank the entire MMS team and instrument leaders for data access and support. This work was supported by the National Natural Science Foundation of China (41374168, 41404132, 41574168, and 41674161) and China Postdoctoral Science Foundation Funded Project (2015T80830). The French participation in the MMS mission was funded by CNES. Data are publicly available from the MMS Science Data Center at http://lasp.colorado.edu/mms/sdc/.

References

Balikhin, M. A., D. G. Sibeck, A. Runov, and S. N. Walker (2012), Magnetic holes in the vicinity of dipolarization fronts: Mirror or tearing structures, *J. Geophys. Res.*, *117*, A08229, doi:10.1029/2012JA017552.

Burch, J. L., et al. (2015), Magnetospheric multiscale overview and science objectives, *Space Sci. Rev.*, *199*, 5–21, doi:10.1007/s11214-015-0164-9.

Baumgärtel, K. (1999), Soliton approach to magnetic holes, *J. Geophys. Res.*, *104*, 28,295–28,308, doi:10.1029/1999JA900393.

Breuillard, H., E. Yordanova, A. Vaivads, and O. Alexandrova (2016), The effects of kinetic instabilities on small-scale turbulence in Earth's magnetosheath, *Astrophys. J.*, *829*, 54, doi:10.3847/0004-637X/829/1/54.

Burlaga, L. F., and J. F. Lemaire (1978), Interplanetary magnetic holes: Theory, *J. Geophys. Res.*, *83*, 5157–5160, doi:10.1029/JA083iA11p05157.

Chisham, G., S. J. Schwartz, M. A. Balikhin, and M. W. Dunlop (1999), AMPTE observations of mirror mode waves in the magnetosheath: Wave vector determination, *J. Geophys. Res.*, *104*, 437–447, doi:10.1029/1998JA900044.

Fazakerley, A. N., and D. J. Southwood (1994), Mirror instability in the magnetosheath, *Adv. Space Res.*, *14*, 65–68.

Gary, S. P., and H. Karimabadi (2006), Linear theory of electron temperature anisotropy instabilities: Whistler, mirror, and Weibel, *J. Geophys. Res.*, *111*, A11224, doi:10.1029/2006JA011764.

Ge, Y. S., J. P. McFadden, J. Raeder, V. Angelopoulos, D. Larson, and O. D. Constantinescu (2011), Case studies of mirror-mode structures observed by THEMIS in the near-Earth tail during substorms, *J. Geophys. Res.*, *116*, A01209, doi:10.1029/2010JA015546.

Gershman, D. J., et al. (2016), Electron dynamics in a subproton-gyroscale magnetic hole, *Geophys. Res. Lett.*, *43*, 4112–4118, doi:10.1002/2016GL068545.

Goodrich, K. A., et al. (2016), MMS multipoint electric field observations of small-scale magnetic holes, *Geophys. Res. Lett.*, *43*, 5953–5959, doi:10.1002/2016GL069157.

Hasegawa, A. (1969), Drift mirror instability in the magnetosphere, *Phys. Fluids*, *12*, 2642–2650, doi:10.1063/1.1692407.

Haynes, C. T., D. Burgess, E. Camporeale, and T. Sundberg (2015), Electron vortex magnetic holes: A nonlinear coherent plasma structure, *Phys. Plasmas*, *22*, 012309, doi:10.1063/1.4906356.

He, J.-S., E. Marsch, C.-Y. Tu, Q.-G. Zong, S. Yao, and H. Tian (2011), Two-dimensional correlation functions for density and magnetic field fluctuations in magnetosheath turbulence measured by the Cluster spacecraft, *J. Geophys. Res.*, *116*, A06207, doi:10.1029/2010JA015974.

Horbury, T. S., E. A. Lucek, A. Balogh, I. Dandouras, and H. Rème (2004), Motion and orientation of magnetic field dips and peaks in the terrestrial magnetosheath, *J. Geophys. Res.*, *109*, A09209, doi:10.1029/2003JA010237.

Huang, S. Y., et al. (2012), Observations of turbulence within reconnection jet in the presence of guide field, *Geophys. Res. Lett.*, *39*, L11104, doi:10.1029/2012GL052210.

Huang, S. Y., F. Sahraoui, X. H. Deng, J. S. He, Z. G. Yuan, M. Zhou, Y. Pang, and H. S. Fu (2014), Kinetic turbulence in the terrestrial magnetosheath: Cluster observations, *Astrophys. J. Lett.*, *789*, L28, doi:10.1088/2041-8205/789/2/L28.

Huang, S. Y., et al. (2016), MMS observations of ion-scale magnetic island in the magnetosheath turbulent plasma, *Geophys. Res. Lett.*, *43*, 7850–7858, doi:10.1002/2016GL070033.

Huang, S. Y., L. Z. Hadid, F. Sahraoui, Z. G. Yuan, and X. H. Deng (2017a), On the existence of the Kolmogorov inertial range in the terrestrial magnetosheath turbulence, *Astrophys. J. Lett.*, *836*, L10, doi:10.3847/2041-8213/836/1/L10.

Huang, S. Y., et al. (2017b), Magnetospheric Multiscale observations of electron vortex magnetic hole in the turbulent magnetosheath plasma, *Astrophys. J. Lett.*, *836*, L27, doi:10.3847/20418213/aa5f50.

Karimabadi, H., et al. (2014), The link between shocks, turbulence, and magnetic reconnection in collisionless plasmas, *Phys. Plasmas*, *21*, 062308, doi:10.1063/1.4882875.

Ji, X.-F., X.-G. Wang, W.-J. Sun, C.-J. Xiao, Q.-Q. Shi, J. Liu, and Z.-Y. Pu (2014), EMHD theory and observations of electron solitary waves in magnetotail plasmas, *J. Geophys. Res. Space Physics*, *119*, 4281–4289, doi:10.1002/2014JA019924.

Li, Z.-Y., W.-J. Sun, X.-G. Wang, Q.-Q. Shi, C.-J. Xiao, Z.-Y. Pu, X.-F. Ji, S.-T. Yao, and S.-Y. Fu (2016), An EMHD soliton model for small-scale magnetic holes in magnetospheric plasmas, *J. Geophys. Res. Space Physics*, *121*, 4180–4190, doi:10.1002/2016JA022424.

Pollock, C., et al. (2016), Fast plasma investigation for magnetospheric multiscale, *Space Sci. Rev.*, *199*, 331, doi:10.1007/s11214-016-0245-4.

Pokhotelov, O. A., O. G. Onishchenko, and L. Stenflo (2013), Physical mechanisms for electron mirror and field swelling modes, *Phys. Scr.*, *87*(6), 065303.

Retinò, A., D. Sundkvist, A. Vaivads, F. Mozer, M. André, and C. J. Owen (2007), In situ evidence of magnetic reconnection in turbulent plasma, *Nat. Phys.*, *3*, 236–238.

Russell, C. T., L. K. Jian, J. G. Luhmann, T. L. Zhang, F. M. Neubauer, R. M. Skoug, X. Blanco-Cano, N. Omidi, and M. M. Cowee (2008), Mirror mode waves: Messengers from the coronal heating region, *Geophys. Res. Lett.*, *35*, L15101, doi:10.1029/2008GL034096.

Russell, C. T., et al. (2016), The magnetospheric multiscale magnetometers, *Space Sci. Rev.*, doi:10.1007/s11214-014-0057-3.

Roytershteyn, V., H. Karimabadi, and A. Roberts (2015), Generation of magnetic holes in fully kinetic simulations of collisionless turbulence, *Phil. Trans. R. Soc. A*, *373*(20), 140–151, doi:10.1098/rsta.2014.0151.

Sahraoui, F., et al. (2003), ULF wave identification in the magnetosheath: The k-filtering technique applied to Cluster II data, *J. Geophys. Res.* *108*(A9), 1335, doi:10.1029/2002JA009587.

Sahraoui, F., G. Belmont, J. L. Pinçon, L. Rezeau, A. Balogh, P. Robert, and N. Cornilleau-Wehrlin (2004), Magnetic turbulent spectra in the magnetosheath: New insights, *Ann. Geophys.*, *22*, 2283–2288, doi:10.5194/angeo-22-2283-2004.

Sahraoui, F., G. Belmont, L. Rezeau, and N. Cornilleau-Wehrlin (2006), Anisotropic turbulent spectra in the terrestrial magnetosheath as seen by the Cluster spacecraft, *Phys. Rev. Lett.*, *96*, 075002.

Shi, Q. Q., et al. (2009), Spatial structures of magnetic depression in the Earth's high-altitude cusp: Cluster multipoint observations, *J. Geophys. Res.*, *114*, A10202, doi:10.1029/2009JA014283.

Stasiewicz, K. (2004), Theory and observations of slow-mode solitons in space plasmas, *Phys. Rev. Lett.*, *93*, 125,004, doi:10.1103/PhysRevLett.93.125004.

Stasiewicz, K., P. K. Shukla, G. Gustafsson, S. Buchert, B. Lavraud, B. Thidé, and Z. Klos (2003), Slow magnetosonic solitons detected by the Cluster spacecraft, *Phys. Rev. Lett.*, *90*, 085002, doi:10.1103/PhysRevLett.90.085002.

Sonnerup, B. U. O., and M. Scheible (1998), Minimum and maximum variance analysis, in *Analysis Methods for Multi-spacecraft Data*, *no. SR-001 in ISSI Scientific Reports*, edited by G. Paschmann and P. W. Daly, chap. 1, pp. 185–220, ESA Publ. Div, Noordwijk, Netherlands.

Sun, W. J., et al. (2012), Cluster and TC-1 observation of magnetic holes in the plasma sheet, *Ann. Geophys.*, *30*, 583–595, doi:10.5194/angeo-30-583-2012.

Sundberg, T., D. Burgess, and C. T. Haynes (2015), Properties and origin of subproton-scale magnetic holes in the terrestrial plasma sheet, *J. Geophys. Res. Space Physics*, *120*, 2600–2615, doi:10.1002/2014JA020856.

Tsurutani, B. T., E. J. Smith, R. R. Anderson, K. W. Ogilvie, J. D. Scudder, D. N. Baker, and S. J. Bame (1982), Lion roars and nonoscillatory drift mirror waves in the magnetosheath, *J. Geophys. Res.*, *87*, 6060–6072, doi:10.1029/JA087iA08p06060.

Tsurutani, B. T., B. Dasgupta, C. Galvan, M. Neugebauer, G. S. Lakhina, J. K. Arballo, D. Winterhalter, B. E. Goldstein, and B. Buti (2002), Phase-steepened Alfvén waves, proton perpendicular energization and the creation of magnetic holes and magnetic decreases: The ponderomotive force, *Geophys. Res. Lett.*, *29*(24), 2233, doi:10.1029/2002GL015652.

Tsurutani, B. T., G. S. Lakhina, J. S. Pickett, F. L. Guarnieri, N. Lin, and B. E. Goldstein (2005), Nonlinear Alfveń waves, discontinuities, proton perpendicular acceleration, and magnetic holes/decreases in interplane- tary space and the magnetosphere: Intermediate shocks?, *Nonlinear Processes Geophys.*, *12*, 321–336, doi:10.5194/npg-12-321-2005.

Tsurutani, B. T., G. S. Lakhina, O. P. Verkhoglyadova, E. Echer, F. L. Guarnieri, Y. Narita, and D. O. Constantinescu (2011), Magnetosheath and heliosheath mirror mode structures, interplanetary magnetic decreases, and linear magnetic decreases: Differences and distinguishing features, *J. Geophys. Res.*, *116*, A02103, doi:10.1029/2010JA015913.

Turner, J. M., L. F. Burlaga, N. F. Ness, and J. F. Lemaire (1977), Magnetic holes in the solar wind, *J. Geophys. Res.*, *82*, 1921–1924, doi:10.1029/JA082i013p01921.

Violante, L., M. B. Bavassano Cattaneo, G. Moreno, and J. D. Richardson (1995), Observations of mirror waves and plasma depletion layer upstream of Saturn's magnetopause, *J. Geophys. Res.*, *100*, 12,047–12,055, doi:10.1029/94JA02703.

Yao, S. T., et al. (2016), Propagation of small size magnetic holes in the magnetospheric plasma sheet, *J. Geophys. Res. Space Physics*, *121*, 5510–5519, doi:10.1002/2016JA022741.

Yao, S. T., et al. (2017), Observations of kinetic-size magnetic holes in the mag- netosheath, *J. Geophys. Res. Space Physics*, *122*, doi:10.1002/2016JA023858.

Yordanova, E., A. Vaivads, M. André, S. C. Buchert, and Z. Vörös (2008), Magnetosheath plasma turbulence and its spatiotemporal evolution as observed by the Cluster spacecraft, *Phys. Rev. Lett.*, *100*(20), 205003.

Zhang, T. L., et al. (2008), Characteristic size and shape of the mirror mode structures in the solar wind at 0.72 AU, *Geophys. Res. Lett.*, *35*, L10106, doi:10.1029/2008GL033793.

Zhang, T. L., W. Baumjohann, C. T. Russell, L. K. Jian, C. Wang, J. B. Cao, M. Balikhin, X. Blanco-Cano, M. Delva, and M. Volwerk (2009), Mirror mode structures in the solar wind at 0.72 AU, *J. Geophys. Res.*, *114*, A10107, doi:10.1029/2009JA014103.